View metadata, citation and similar papers at core.ac.uk
brought to you by CORE
provided by Open Access LMU

Original Article

JCBFM

Journal of Cerebral Blood Flow & Metabolism
2017, Vol. 37(11) 3625–3634
© Author(s) 2017
Reprints and permissions:
sagepub.co.uk/journalsPermissions.nav
DOI: 10.1177/0271678X16686595
journals.sagepub.com/home/jcbfm
SAGE

Inversion of neurovascular coupling after subarachnoid hemorrhage in vivo

Matilde Balbi[1,2], Masayo Koide[3], George C Wellman[3] and Nikolaus Plesnila[1,2,4]

Abstract

Subarachnoid hemorrhage (SAH) induces acute changes in the cerebral microcirculation. Recent findings ex vivo suggest neurovascular coupling (NVC), the process that increases cerebral blood flow upon neuronal activity, is also impaired after SAH. The aim of the current study was to investigate whether this occurs also in vivo. C57BL/6 mice were subjected to either sham surgery or SAH by filament perforation. Twenty-four hours later NVC was tested by forepaw stimulation and CO_2 reactivity by inhalation of 10% CO_2. Vessel diameter was assessed in vivo by two-photon microscopy. NVC was also investigated ex vivo using brain slices. Cerebral arterioles of sham-operated mice dilated to 130% of baseline upon CO_2 inhalation or forepaw stimulation and cerebral blood flow (CBF) increased. Following SAH, however, CO_2 reactivity was completely lost and the majority of cerebral arterioles showed paradoxical constriction in vivo and ex vivo resulting in a reduced CBF response. As previous results showed intact NVC 3 h after SAH, the current findings indicate that impairment of NVC after cerebral hemorrhage occurs secondarily and is progressive. Since neuronal activity-induced vasoconstriction (inverse NVC) is likely to further aggravate SAH-induced cerebral ischemia and subsequent brain damage, inverse NVC may represent a novel therapeutic target after SAH.

Keywords

Subarachnoid hemorrhage, neurovascular coupling, CO_2 reactivity, in vivo, paradoxical vasoconstriction

Received 19 September 2016; Revised 2 December 2016; Accepted 5 December 2016

Introduction

Subarachnoid hemorrhage (SAH) is a subtype of hemorrhagic stroke responsible for 6 to 10% of all stroke events.[1] Due to its high mortality rate of almost 50%, SAH accounts for about 20% of cerebrovascular related deaths.[2] Additionally, 30% of all SAH survivors remain severely disabled.[3] In 85% of cases, SAH is caused by a spontaneous rupture of a cerebral aneurysm located at the base of the skull with subsequent bleeding into the subarachnoid space. As a consequence of hematoma formation, intracranial pressure (ICP) spikes to levels that substantially decrease cerebral perfusion pressure (CPP), causing global cerebral ischemia. Cerebral blood flow (CBF) recovers after a few minutes, only to significantly decrease again within the next few hours.[4] Data from experimental studies directly visualizing cerebral microvessels after SAH have shown that post-hemorrhage ischemia is characterized by persistent spasms of pial arterioles which cause reductions of CBF and thrombus formation resulting in lack of microvascular perfusion.[5–7] Accordingly, basal blood flow is reduced after SAH and may result in ischemic brain damage and bad outcome.

In addition to the basal level of CBF, it is also critically important that cerebral vessels dilate upon activation of nearby neurons in order to match the local delivery of oxygen and glucose to focal increases in metabolic demand within the central nervous system.

[1]Institute for Stroke and Dementia Research (ISD), University of Munich Medical Center, Ludwig-Maximilians University (LMU), Munich, Germany
[2]Graduate School of Systemic Neurosciences (GSN), Ludwig-Maximilians University (LMU), Munich, Germany
[3]Department of Pharmacology, University of Vermont, Burlington, VT, USA
[4]Munich Cluster for Systems Neurology, Munich, Germany

Corresponding author:
Nikolaus Plesnila, Institute for Stroke and Dementia Research (ISD), University of Munich Medical Center, Feodor-Lynen Strasse 17, Munich 81377, Germany.
Email: nikolaus.plesnila@med.uni-muenchen.de

This process, called neurovascular coupling (NVC), was recognized by Moore and Cao[8] and Roy and Sherrington[9] and is mediated by both metabolic agents—e.g. increased CO_2 and decreased pH—as well as complex signaling between neurons, astrocytes, pericytes, and endothelial cells—the so called neurovascular unit. So far, however, very little is known about the consequences of SAH on NVC in vivo.

We recently demonstrated in vivo that within 3 h after SAH pial and parenchymal, microvessels lose their ability to respond to CO_2, while NVC is completely preserved.[10,11] However, when assessing NVC ex vivo in brain slices from SAH-operated rats, we showed a time-dependent impairment/inversion of NVC lasting for up to 96 h after SAH.[12] Since thus far it is unclear whether NVC is also impaired in vivo following SAH, the aim of the current study was to subject mice to SAH and directly visualize the response of their pial and parenchymal vessels upon forepaw stimulation and CO_2 inhalation 24 h after hemorrhage.

Materials and methods

Animal breeding, housing, and all experimental procedures were conducted according to institutional guidelines. Experiments performed at the Institute for Stroke and Dementia Research, University of Munich Medical Center were approved by the Ethical Review Board of the Government of Upper Bavaria (protocol number 136-11). Experiments performed at the Department of Pharmacology, University of Vermont were approved by the Institutional Animal Care and Use Committee at the University of Vermont. Male C57BL/6 mice (20 to 23 g body weight Charles River Laboratory, Sulzfeld, Germany and Charles River Laboratory, Saint Constant, Quebec, Canada) were used for this study. Experiments were planned, carried out, and reported according to the ARRIVE guidelines.[13]

Animal preparation and monitoring

Experimental animals had free access to food and water before and after surgery. For induction of SAH, anesthesia was induced by intraperitoneal injection of midazolam (5 mg/kg; Braun, Melsungen, Germany), fentanyl (0.05 mg/kg; Jansen-Cilag, Neuss, Germany), and medetomidine (0.5 mg/kg; Pfizer, Karlsruhe, Germany) as previously described.[14,15] Mice were orotrachealy intubated and mechanically ventilated (Minivent, Hugo Sachs, Hugstetten, Germany). End-tidal pCO_2 was measured with a microcapnometer (Capnograph, Hugo Sachs, Hugstetten, Germany) and kept constant between 30 and 40 mmHg by respective adjustments to the ventilation. To maintain body temperature at 37°C a thermostatically regulated, feedback-controlled heating pad (FHC, Bowdoin, ME, USA) was used. ICP was measured in each animal for 15 min after SAH using a microsensor-based ICP probe (Codman & Shurteff Inc, Raynham, MA) to prove successful induction of SAH as described before.[16]For continuous monitoring of regional cerebral blood flow (rCBF), a flexible laser-Doppler probe (Periflux 4001 Master, Perimed, Stockholm, Sweden) was glued onto the skull above the territory of the left middle cerebral artery (MCA). Blood gases and electrolytes were measured at the end of each experiment.

For experiments on NVC and vasoreactivity, mice were initially anesthetized with 2% isoflurane in 70% N_2O and 30% O_2. Later on, isoflurane was gradually reduced over the course of 10 min to a range of 0.5 to 0.9% in 70% room air and 30% O_2. At the same time, a continuous intra-arterial infusion of ketamine (30 mg/kg/h, Inresa, Freiburg, Germany) was administered.[17]

Induction of SAH

SAH was induced using the filament perforation model as previously described.[16,18,19] Briefly, a 5–0 monofilament was introduced via the left external carotid artery into the internal carotid artery and advanced intracranially. SAH induction was marked by a sudden increase of ICP. Immediately after, the filament was withdrawn and the external carotid artery was ligated. The same procedure was followed in sham-operated mice with the only exception that the filament was not advanced far enough to induce hemorrhage. Anesthesia was terminated by intraperitoneal injection of atipamezole (2.5 mg/kg; Pfizer) naloxone (1.2 mg/kg; Inresa, Freiburg, Germany), and flumazenil (0.5 mg/kg; Hoffmann-La-Roche, Grenzach-Wyhlen,Germany). Thereafter, mice were kept in an incubator at 33°C for 2.5 h. Identical surgical procedures were used for the induction of SAH in mice used for ex vivo studies with the exception that inhalation of isoflurane (4% induction; 2% maintenance) was used to achieve a surgical plane of anesthesia.

Forepaw-evoked NVC

Mice were re-anesthetized 24 h after SAH and the CBF response after NVC was evaluated as previously described.[11,17] Briefly, the left forepaw was stimulated with two subdermal needle electrodes with a diameter of 0.2 mm (Hwato, Suzhou, China) at an intensity of 2 mA for 0.3 ms (Digitimer Ltd, Hertfordshire, England). One stimulation cycle contained 96 stimulations and lasted for 16 s (6 Hz). The interval between two stimulation cycles was 40 s. CBF was assessed at five different locations covering the whole somatosensory

cortex. The region with the strongest CBF response was also continuously stimulated (2 mA) for 1 min in order to evaluate the response to a tonic stimulus. This region was then considered for analysis and further for assessment of the microvascular response by two-photon microscopy (Figure 1(a)).

Two-photon microscopy

After assessing the CBF response to forepaw stimulation, a cranial window (2 × 1 mm) was drilled under constant cooling above the area of the somatosensory cortex associated to the forepaw leaving the dura mater intact as previously described.[20] Mice were placed under a two-photon microscope (Zeiss LSM-7 MP, Oberkochen, Germany) equipped with a Li:Ti laser (Chameleon, Coherent, USA) as described previously,[21] and the exposed dura mater was kept wet with isotonic saline. The fluorescent plasma dye, fluorescein isothiocyanate (FITC-dextran; molecular weight 150 kDa) was given systematically via femoral artery injection (0.05 ml of a 0.5% solution; Sigma, Deisenhofen, Germany) and all parenchymal (diameter: 5–20 μm; depth: 150 μm) and pial arterioles (diameter: 20 to 40 μm) in the region were visualized using two-photon fluorescence microscopy and a 10 × Zeiss EC Plan-NeoFluar objective. Pial arterioles were followed into the parenchyma along an axis normal to the brain surface. Arterioles were distinguished from venules on the basis of velocity and direction of blood flow.

Vascular reactivity to CO_2

Diameters of both parenchymal and pial arterioles were examined under physiological conditions in order to obtain baseline values. Thereafter, arteriolar diameter was observed during inhalation of 10% CO_2 for 10 min. The amount of inhaled CO_2 was measured by microcapnometry (Hugo-Sachs Elektronik, March-Hugstetten, Germany). Arteriolar diameters were quantified with calibrated image analysis software (Zen, Zeiss, Oberkochen, Germany) and expressed in percentage of baseline as previously described.[17]

Vessel diameter during forepaw-evoked NVC

For evaluation of changes in vessel diameter after forepaw stimulation, the same protocol was used as for assessment of CBF. Briefly, the region previously identified to yield the most pronounced CBF response was activated by forepaw stimulation using a cycle that contained 96 stimulations and lasted for 16 s (6 Hz). The interval between two stimulation cycles was 40 s. Thereafter, the same region was continuously stimulated (2 mA) for 1 min in order to evaluate the response to a tonic stimulus.

NVC ex vivo using freshly prepared brain slices

NVC was examined ex vivo in freshly prepared brain slices obtained from control and 24-h SAH animals. The diameter of parenchymal arterioles was measured

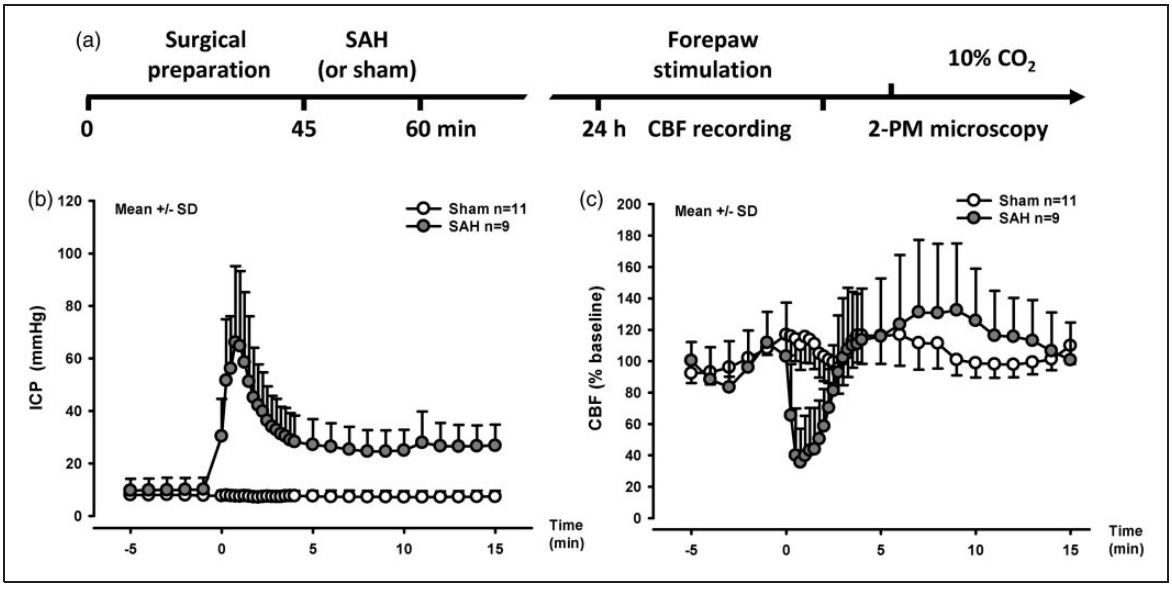

Figure 1. SAH induction and experimental design. (a) Schematic representation of the experimental design for both SAH and sham surgery and forepaw stimulation followed by 10% CO_2 inhalation. (b) Intracranial pressure and (c) cerebral blood flow starting 5 min before SAH induction and continuing for the first 15 min after arterial perforation. A sudden increase in ICP and drop in CBF confirm vessel perforation. Mean ± SD; n = 11 in sham and n = 9 in SAH group.

by infrared-differential interference contrast (IR-DIC) microscopy as previously described.[12,22] Briefly, brains were dissected from mice after decapitation under deep pentobarbital anesthesia (60 mg/kg) and sliced into 160 μm thick cortical slices from the MCA territory using Leica VT1000S vibratome. Brain slices were perfused with artificial cerebral spinal fluid (aCSF; 125 mM NaCl, 3 mM KCl, 18 mM $NaHCO_3$, 1.25 mM NaH_2PO_4, 1 mM $MgCl_2$, 2 mM $CaCl_2$, 5 mM glucose and 0.4 mM ascorbic acid, aerated with 5% CO_2/20% O2/75% N2, pH 7.35, 35–37°C) throughout the experiment. The thromboxane A_2 analog, U46619 (125 nM, Calbiochem), was added to aCSF to establish a similar level of arteriolar tone in slices from both animal groups. Arteriolar diameter before EFS were 4.28 ± 0.35 μm (control) and 4.59 ± 0.20 μm (SAH 24 h), and not significantly different between groups. NVC was initiated using electrical field stimulation (EFS, 50 Hz, 0.3-ms alternating square pulse, 3-s duration). IR-DIC images (820 nm) were acquired at ~1 Hz using a Biorad Radiance multiphoton imaging system, and arteriolar diameter was measured at three points along the segment (~10 μm) of the arteriole exhibiting the largest response to EFS by SparkAn image analysis software (written by Dr. Bonev, Univeristy of Vermont).

Statistical analysis

For in vivo studies, statistical analysis was performed with a standard statistical software package (Sigma Plot 12.5; Systat Software, Erkrath, Germany). Results for CO_2 reactivity experiments are presented as mean ± standard error of the mean (SEM). Results for somatosensory stimulation are presented as median ± 75/25 percentile. Differences across groups were evaluated using the Mann–Whitney Rank Sum test with the Bonferroni correction. For the ex vivo study, Origin 9.1 software (Origin Lab, Northampton, MA, USA) was used for statistical analysis. EFS-induced changes in arteriolar diameter are expressed as percent change in diameter (mean ± SEM) and were evaluated by unpaired *t*-test.

Randomization and blinding

All animals were randomly assigned to the procedures; the surgical preparation and data analysis were performed by a researcher blinded towards the treatment of the animals.

Results

In vivo physiological parameters and mortality

All physiological parameters—body temperature, systemic blood pressure, blood pH, pCO_2 and pO_2—factors shown to effect CBF[23] were carefully monitored during the procedure and did not differ between groups (Supplementary table 1). When SAH was induced, the resulting increased ICP caused a reduction in CPP and a reduction of CBF of approximately 85%. After ICP decreased to values around 30 mmHg, CBF stabilized and remained constant for the remainder of the observation period (Figure 1(b) to (c)). Two mice from each group (4 out of 21) died before imaging could be performed, and another mouse died during procedures after CBF recording.

In vivo CO_2 reactivity in cerebral pial arteries and parenchymal arterioles is abolished 24 h following SAH

Direct visualization of pial and parenchymal vessels with two-photon microscopy showed a compromised endothelium-dependent response after SAH. In sham-operated mice, pial arterioles dilated upon inhalation of 10% CO_2 (Figure 2(a) and (b) white symbols). After SAH, however, arteries constricted rather than dilated in response to CO_2 inhalation (Figure 2(a) and (b), gray symbols). Considering the important role of the microcirculation in the maintenance of CBF, we also investigated CO_2 responsiveness of parenchymal arterioles. At a depth of about 150 μm into the somatosensory cortex arterioles in the sham-operated mice dilated by >20% in response to inhalation of 10% CO_2 (Figure 2(a) and (c) white symbols). Following SAH parenchymal arterioles showed only an initial increase in diameter of about 10% in response to inhaled CO_2 and then failed maintaining this response over time. We even observed a gradual decline in dilation until vessel diameter returned to baseline values despite continued inhalation of CO_2 (Figure 2(d) and (e), gray symbols). These results demonstrate that the vasodilation observed in healthy mice in response to CO_2 exposure is dramatically abolished in pial and parenchymal arterioles after SAH. Moreover, these data indicate that the severe endothelium-dependent dysfunction that we previously observed 3 h after SAH [11] remains 24 h after the initial bleeding.

In vivo NVC is compromised 24 hours after SAH

Twenty-four hours after hemorrhage, the increase of CBF in response to repetitive sensory stimulation of the forepaw was comparable between sham-operated and SAH mice (Figure 3(a) to (c)). A stronger, continuous sensory stimulation of the forepaw for 1 min, however, increased CBF only in sham-operated mice (Figure 3(d) to (e), white symbols), while the response in SAH mice was significantly attenuated (Figure 3(d) to (e), gray symbols).

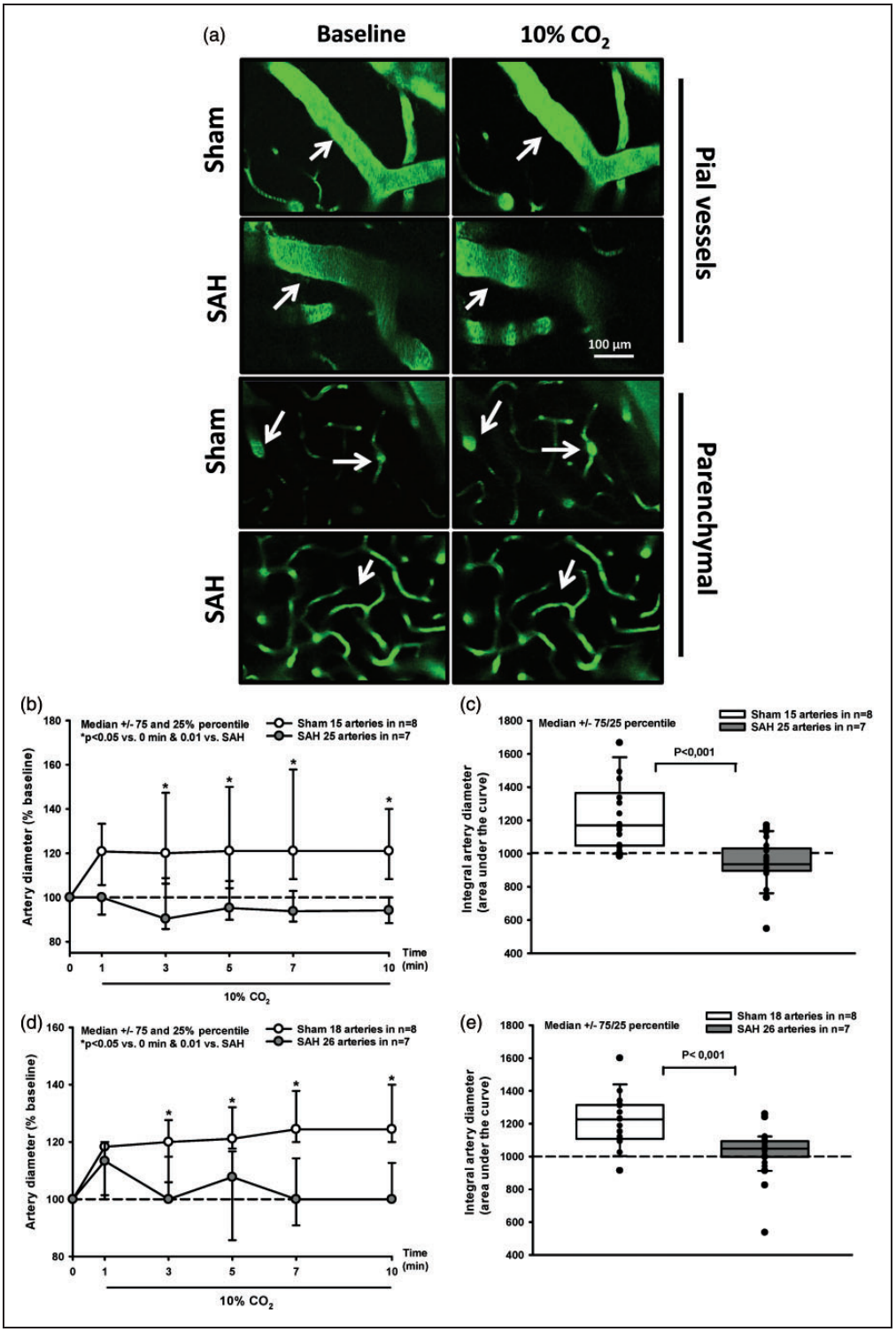

Figure 2. Pial and parenchymal arteries do not respond to hypercapnia 24 h after SAH. (a) Representative two-photon microscopy images of pial (top) and parenchymal arterioles (bottom) of SAH and sham-operated mice before and during 10% CO_2 inhalation. (b) Surface and (d) parenchymal artery diameter during hypercapnia of mice subjected to sham surgery (white symbols) or SAH (gray symbols). Pial and parenchymal vessel dilated normally in response to inhalation of 10% CO_2 in sham-operated mice (white symbols), while no response was observed after SAH (gray symbols). (c–e) Box plots show the quantification of the integral artery diameter that corresponds to the area under the curve.

Mean ± SEM; Mann–Whitney Rank Sum test ($P < 0.05$ vs. 0 min and $P < 0.01$ vs. SAH). Median ± 75/25 percentile; Mann–Whitney Rank Sum test ($P < 0.001$). 15 to 25 arteries (b–c) and 18 to 26 arteries (d–e) in n = 7 to 8 mice per group.

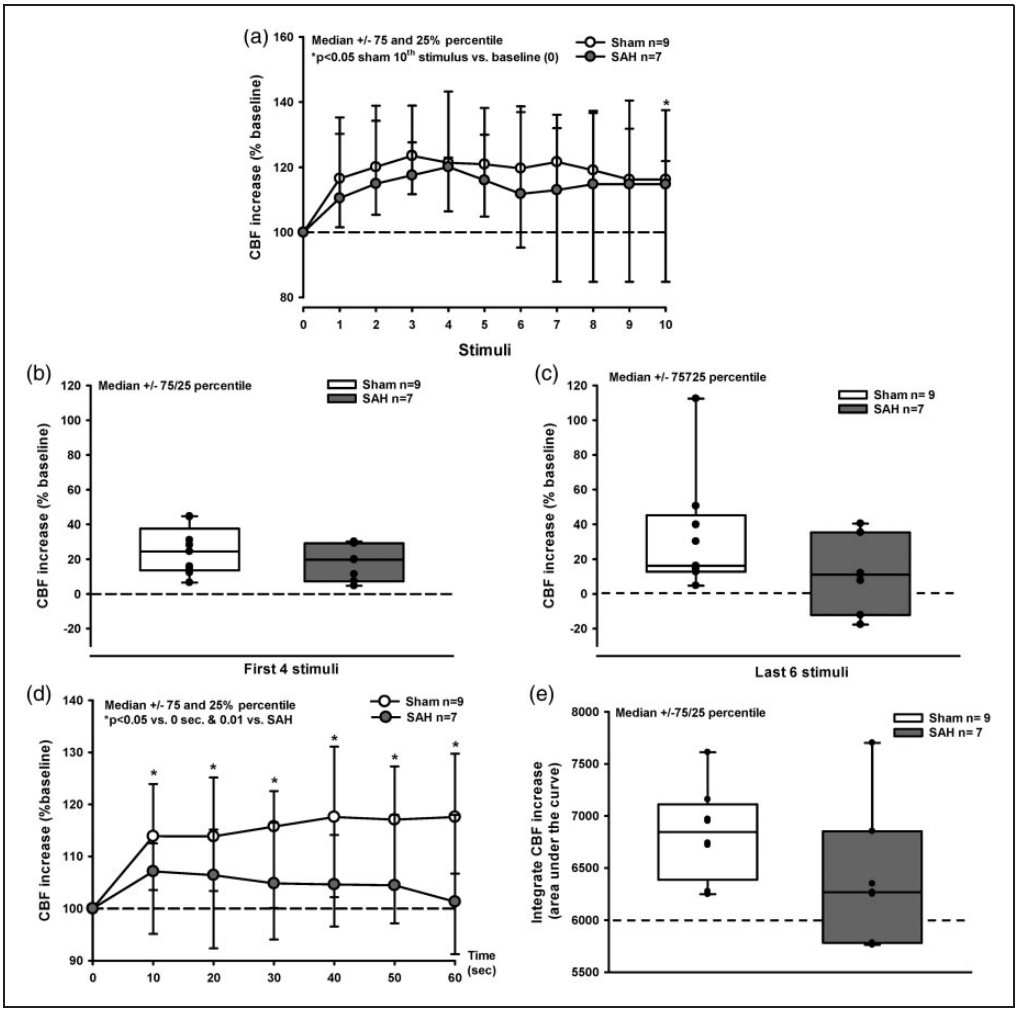

Figure 3. Changes in CBF in response to neurovascular coupling 24 h after SAH. (a) Sensory stimulation to 10 consecutive stimuli shows an increase in CBF response that attenuates in SAH mice until it becomes statistically significant from the response in sham mice at the 10th stimulus. (b–c) Box plots showing CBF increase in response to the first four (b) and last six (c) discrete electrical stimuli to the forepaw, in sham-operated mice (white symbols) and after SAH (gray symbols). No significant effect was found between the experimental groups. (d–e) CBF increase in response to continuous electrical stimulation shows a significant difference between sham-operated mice and mice subjected to SAH, though this is not apparent when quantifying the area under the curve (e). Mean ± SEM; Mann–Whitney Rank Sum test ($P < 0.05$ vs. 0 s and $P < 0.01$ vs. SAH). Median ± 75/25 percentile. n = 7 to 9 per group.

Visualization of parenchymal arterioles of up to 20 µm in diameter in response to repetitive forepaw stimulation showed a similar picture. Stimulation caused an increase in parenchymal arteriolar diameter in the sham-operated group of about 20% (Figure 4(a) to (c), white symbols). After SAH, this response was absent; even a tendency towards inversion of NVC was observed (Figure 4(a) to (c), gray symbols). When using a stronger stimulation paradigm, i.e. continuous forepaw stimulation for 1 min, this response became more evident. Arterioles dilated by 25% in sham-operated animals (Figure 4(d) and (e), white symbols), but massive and significant arterial constriction was observed in SAH mice (Figure 4(d) and (e), gray symbols). These results demonstrate a severe dysfunction of NVC 24 h after SAH in vivo.

Inversion of NVC in brain slices from 24-hour SAH animals

We have previously reported that ex vivo NVC was preserved (i.e. EFS-induced vasodilation) in the acute phase (first 3 to 4 h) of SAH in both rat[22] and mouse SAH model animals.[11] Here, we have examined ex vivo NVC in brain slices obtained from 24-h SAH model mice. As previously shown, focal neuronal activation by EFS led to arteriolar dilation in brain slices from un-operated control animals (20.8 ± 1.7% increase in

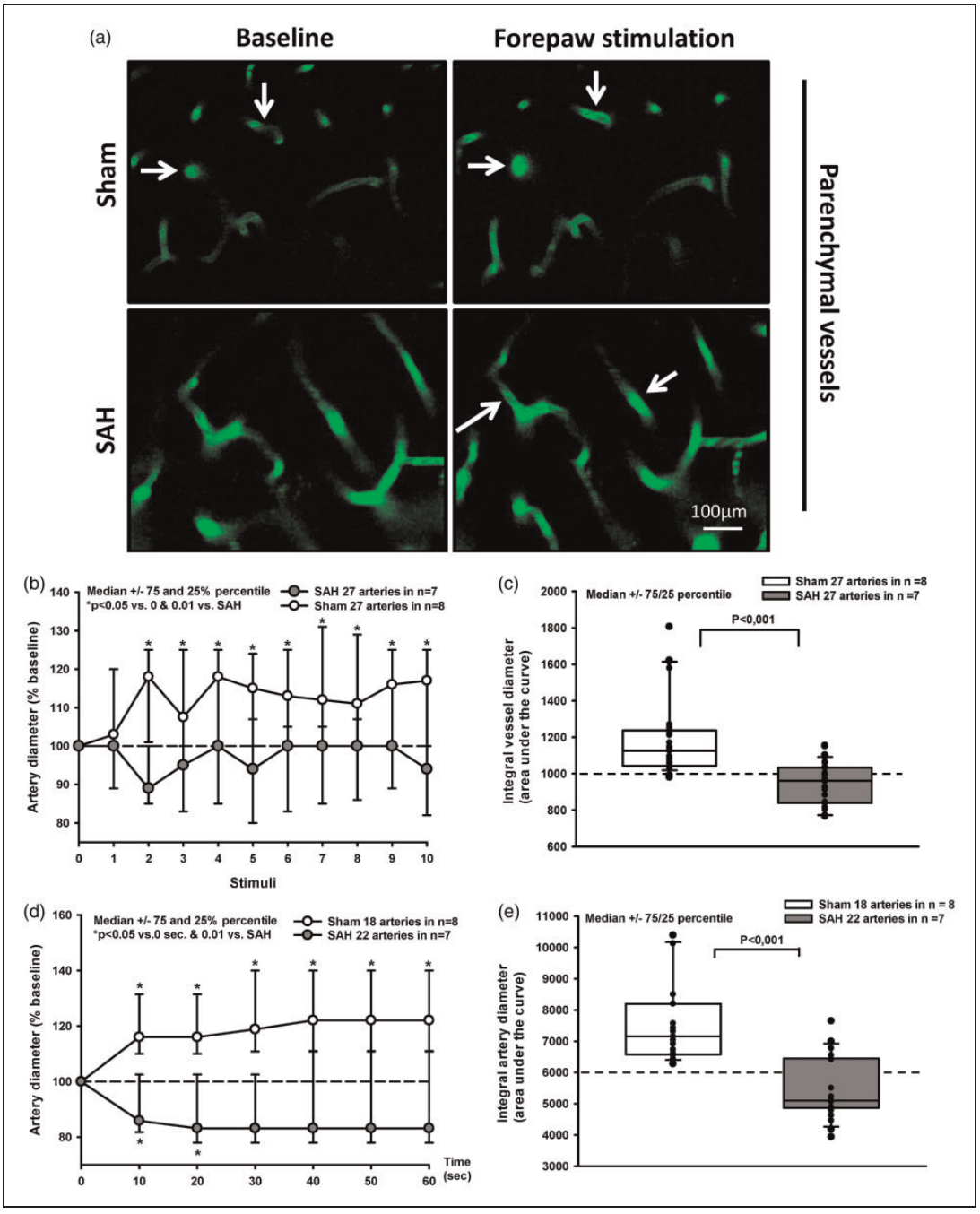

Figure 4. Two-photon imaging of arteriolar diameter demonstrates severe impairment of neurovascular coupling 24 h after SAH. (a) Representative two-photon microscopy image of parenchymal vessel in sham-operated mice (top) and SAH mice (bottom) at baseline and after stimulation. (b–c) Arteriolar dilation in response to a discrete electrical stimulation shows a significant difference between experimental groups in the mean change in diameter (b) and the quantification of the integral of arteriolar diameter (c). (d–e) Arteriole dilation in response to a continuous electrical stimulation shows a significant difference between SAH or sham-operated mice. Mean ± SEM; Mann–Whitney Rank Sum test ($P < 0.05$ vs. 0 min and $P < 0.01$ vs. SAH). Median ± 75/25 percentile; Mann–Whitney Rank Sum test. 27 arterioles (b–c) 18 to 22 arterioles (D-C) in n = 7 to 8 mice per group.

diameter, n = 6). By contrast, EFS caused arteriolar constriction in the majority of brain slices from 24-h SAH animals (five out six arterioles, ~83%). On average, EFS caused a constriction representing a decrease in diameter of 16.1 ± 6.1% (n = 6) in brain slices from the 24-h SAH group that was significantly different from the dilation observed in the control group (Figure 5(a)). Individual arteriolar responses to EFS

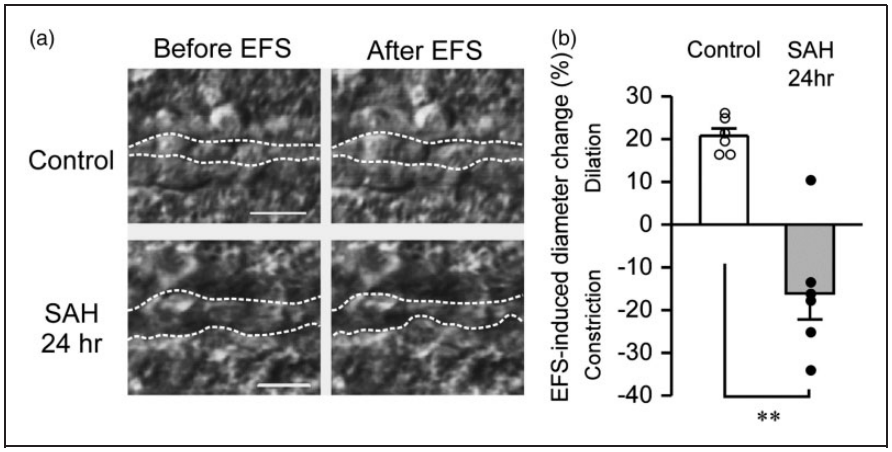

Figure 5. EFS-induced vasoconstriction in brain slices 24 h after SAH. (a) Infrared-differential interference contrast (IR-DIC) images of cortical brain slices from control and 24 h SAH mice, showing inversion of neurovascular coupling 24 h after SAH. EFS induced vasodilation in brain slices from control animals (six out of six arterioles). However, in brain slices obtained from animals 24 h after SAH, EFS caused marked vasoconstriction in five out of six brain slices. Dashes outline the intraluminal diameter of parenchymal arterioles. Scale bars, 10 μm. (b) Summary of EFS-evoked changes in arteriolar diameter in brain slices from control and 24 h SAH animals (n = 6 each). Opened (control) and closed (24 h SAH) circles represent individual data points. Bar graph expresses mean percent change in diameter ± SEM. ** $P < 0.01$, unpaired *t*-test.

are shown in Figure 5(b). Consistent with in vivo observations (Figure 4), these results demonstrate ex vivo inversion of NVC 24 h after SAH.

Discussion

Based on our previous work investigating NVC within the first few hours after SAH, the aim of our current investigation was to examine how in vivo and ex vivo neurovascular communication evolves over time after SAH. In order to do so, we used two-photon microscopy to visualize reactivity of both pial and parenchymal vessels 24 h after induction of SAH in mice. Our data show that after SAH, cerebral vessels across the vascular tree—pial and parenchymal arteries—fail to dilate in response to CO_2, which is a vasoactive metabolic byproduct that specifically dilates cerebral vessels.[24,25] Moreover, our data show a delayed dysfunction in NVC in vivo as well as ex vivo, with an inverse response 24 h after SAH, indicating that after SAH, neuronal activity constricts rather than dilates cerebral vessels.

Severe endothelium-dependent dysfunction in vivo was identified for the first time by direct observation of pial vessels 3 and 24 h after SAH using conventional epi-fluorescence microscopy.[10,26,27] However, due to the limited penetration depth of the technology used in these studies, the investigation was limited to vessels on the brain surface. This limitation was overcome using two-photon microscopy, to provide the first in vivo measurements of parenchymal arteriolar functionality 3 h after SAH.[11] It was found that in addition to microvessels located on the brain surface, arterioles in the parenchyma lost their ability to dilate in response to CO_2 inhalation. This study investigated the very acute phase after hemorrhage (i.e. 3 h) when vasospasm occurs in microvessels; however, it remained unclear if this process was short-lived or if it persisted beyond the acute phase of SAH. In the current study, we show that this early loss of CO_2 reactivity in pial and parenchymal vessels persists for at least 24 h after hemorrhage. The relevance of this finding is that following SAH, the brain seems to be unable to adjust blood flow to neuronal activity. Hence, each firing of neurons causes a mismatch of flow and metabolism and may therefore further damage the brain. Mechanistically, the results of the current study suggest that endothelial NO signaling may be dysfunctional after SAH. This is based on the observation that CO_2 reactivity is at least partially dependent on constitutive endothelial NOS, findings consistent with studies showing that during SAH, NO concentration, and eNOS activity drop with the onset of hemorrhage.[28,29]

Importantly, we also show that following hemorrhage, the mechanisms of communication between neurons and vessels that in healthy conditions lead to a balanced supply of oxygen and nutrients to the brain via the blood stream are severely altered 24 h after SAH. Recent ex vivo studies investigating intraparenchymal arterioles in rats after SAH reported an inversion of NVC: arterioles constricted rather than dilated in response to neuronal activity 24 to 96 h after SAH.[30] While our previous study investigating neurovascular reactivity showed that NVC is not impaired within the first few hours after SAH,[11] in

the current study, we unequivocally demonstrate in vivo and ex vivo a progression in vascular dysfunction, affecting NVC 24 h after SAH. These findings define a therapeutic time window that could lead to an improvement in the outcome of already promising approaches like NO-based strategies, i.e. administration of inhaled NO[20] or NO donors.[31]

From a mechanistic point of view, recent studies in rat brain slices have provided evidence for a link between SAH-induced inversion of NVC from vasodilation to vasoconstriction and high-amplitude spontaneous calcium (Ca^{2+}) events within astrocytic end-feet, shown to occur only in the end-feet surrounding arterioles that exhibited an inverted response. These changes in signaling have been shown to be causal to the switch in polarity of NVC after SAH.[22] Additionally, the percentage of these end-foot high-amplitude Ca^{2+} signals paralleled the development of the switch in polarity in a time-dependent manner, further corroborating the existence of a therapeutic time window. Broad-spectrum inhibition of purinergic (P2) receptors and targeted inhibition of G_q-coupled P2Y receptors have been shown to abolish high-amplitude Ca^{2+} signals after SAH, but the purine nucleotides responsible were shown not to be released by neurotransmission after SAH.[32] This suggests that the therapeutic targeting of purinergic signaling in astrocytes could be complementary to an early rescue of NO reactivity.

In summary, the current study demonstrates that pial and parenchymal cerebral vessels lose their ability to respond to metabolic stimuli like CO_2 after hemorrhage. Further on, NVC is inversed 24 h after SAH, i.e. neuronal activation results in vasoconstriction instead of vasodilatation. Together with our previous findings showing no impairment of NVC 3 h after SAH, the current results indicate progressive vascular dysfunction following cerebral hemorrhage. Accordingly, the current study provides the first information on the functional integrity of parenchymal microvessels after SAH in vivo. The clinical relevance of our results is that any neuronal activation, e.g. by sensory stimulation, may result in vasoconstriction, mismatch of metabolism and blood flow, relative ischemia, and further damage in SAH patients. Accordingly, SAH patients may need to be handled with special attention until proper neurovascular function is restored or respective therapies are developed to prevent post-hemorrhagic dysfunction of cerebral vessels.

Funding

The author(s) disclosed receipt of the following financial support for the research, authorship, and/or publication of this article: This work was supported by the Solorz-Żak foundation, by the American Heart Association (14SDG20150027), National Institutes of Health (P01 HL095488, P30 RR032135, P30 GM103498 and S10 OD10583), Totman Medical Research Trust Fund, the Peter Martin Brain Aneurysm Endowment, and the Deutsche Forschungsgemeinschaft through the Munich Cluster of Systems Neurology (Synergy).

Declaration of conflicting interests

The author(s) declared no potential conflicts of interest with respect to the research, authorship, and/or publication of this article.

Authors' contributions

MB: performed all in vivo experiments and wrote the manuscript. MK: performed all ex vivo experiments and wrote the manuscript. GCW: designed the study, wrote and edited the manuscript. NP: designed the study, wrote and edited the manuscript.

Supplementary material

Supplementary material for this paper can be found at http://jcbfm.sagepub.com/doi/suppl/10.1177/0271678X16686595

References

1. Cahill J and Zhang JH. Subarachnoid hemorrhage: Is it time for a new direction? *Stroke* 2009; 40: S86–S87.
2. Weaver JP and Fisher M. Subarachnoid hemorrhage: An update of pathogenesis, diagnosis and management. *J Neurol Sci* 1994; 125: 119–131.
3. Van Gijn J and Rinkel GJ. Subarachnoid haemorrhage: Diagnosis, causes and management. *Brain* 2001; 124: 249–278.
4. Schubert GA, Seiz M, Hegewald AA, et al. Acute hypoperfusion immediately after subarachnoid hemorrhage: A xenon contrast-enhanced CT study. *J Neurotrauma* 2009; 26: 2225–2231.
5. Friedrich B, Muller F, Feiler S, et al. Experimental subarachnoid hemorrhage causes early and long-lasting microarterial constriction and microthrombosis: An in-vivo microscopy study. *J Cereb Blood Flow Metabolism* 2012; 32: 447–455.
6. Pennings FA, Bouma GJ and Ince C. Direct observation of the human cerebral microcirculation during aneurysm surgery reveals increased arteriolar contractility. *Stroke* 2004; 35: 1284–1288.
7. Uhl E, Lehmberg J, Steiger HJ, et al. Intraoperative detection of early microvasospasm in patients with subarachnoid hemorrhage by using orthogonal polarization spectral imaging. *Neurosurgery* 2003; 52: 1307–1315.
8. Moore CI and Cao R. The hemo-neural hypothesis: On the role of blood flow in information processing. *J Neurophysiol* 2008; 99: 2035–2047.
9. Roy CS and Sherrington CS. On the regulation of the blood-supply of the brain. *J Physiol* 1890; 11: 85–158.
10. Friedrich B, Michalik R, Oniszczuk A, et al. CO2 has no therapeutic effect on early microvasospasm after experimental subarachnoid hemorrhage. *J Cereb Blood Flow Metabolism* 2014; 34: e1–e6.

11. Balbi M, Koide M, Schwarzmaier SM, et al. Acute changes in neurovascular reactivity after subarachnoid hemorrhage in vivo. *J Cereb Blood Flow Metabolism* 2017; 37(1): 178–187.
12. Koide M, Bonev AD, Nelson MT, et al. Inversion of neurovascular coupling by subarachnoid blood depends on large-conductance Ca^{2+}-activated K^+ (BK) channels. *Proc Natl Acad Sci USA* 2012; 109: E1387–E1395.
13. Kilkenny C, Browne W, Cuthill IC, et al. Animal research: Reporting in vivo experiments: the ARRIVE guidelines. *Br J Pharmacol* 2010; 160: 1577–1579.
14. Thal SC and Plesnila N. Non-invasive intraoperative monitoring of blood pressure and arterial pCO_2 during surgical anesthesia in mice. *J Neurosci Methods* 2007; 159: 261–267.
15. Schwarzmaier SM and Plesnila N. Contributions of the immune system to the pathophysiology of traumatic brain injury – Evidence by intravital microscopy. *Front Cell Neurosci* 2014; 8: 358.
16. Feiler S, Friedrich B, Scholler K, et al. Standardized induction of subarachnoid hemorrhage in mice by intracranial pressure monitoring. *J Neurosci Methods* 2010; 190: 164–170.
17. Balbi M, Ghosh M, Longden TA, et al. Dysfunction of mouse cerebral arteries during early aging. *J Cereb Blood Flow Metabolism* 2015; 35: 1445–1453.
18. Scholler K, Feiler S, Anetsberger S, et al. Contribution of bradykinin receptors to the development of secondary brain damage after experimental subarachnoid hemorrhage. *Neurosurgery* 2011; 68: 1118–1123.
19. Buhler D, Schuller K and Plesnila N. Protocol for the induction of subarachnoid hemorrhage in mice by perforation of the Circle of Willis with an endovascular filament. *Transl Stroke Res* 2014; 5: 653–659.
20. Terpolilli NA, Kim SW, Thal SC, et al. Inhalation of nitric oxide prevents ischemic brain damage in experimental stroke by selective dilatation of collateral arterioles. *Circ Res* 2012; 110: 727–738.
21. Schwarzmaier SM, Zimmermann R, McGarry NB, et al. In vivo temporal and spatial profile of leukocyte adhesion and migration after experimental traumatic brain injury in mice. *J Neuroinflammation* 2013; 10: 32.
22. Pappas AC, Koide M and Wellman GC. Astrocyte Ca^{2+} signaling drives inversion of neurovascular coupling after subarachnoid hemorrhage. *J Neurosci* 2015; 35: 13375–13384.
23. Faraci FM and Heistad DD. Regulation of the cerebral circulation: Role of endothelium and potassium channels. *Physiol Rev* 1998; 78: 53–97.
24. Iadecola C. Does nitric oxide mediate the increases in cerebral blood flow elicited by hypercapnia? *Proc Natl Acad Sci USA* 1992; 89: 3913–3916.
25. Iadecola C and Zhang F. Nitric oxide-dependent and -independent components of cerebrovasodilation elicited by hypercapnia. *Am J Physiol* 1994; 266: R546–R552.
26. Sun BL, Zheng CB, Yang MF, et al. Dynamic alterations of cerebral pial microcirculation during experimental subarachnoid hemorrhage. *Cell Mol Neurobiol* 2009; 29: 235–241.
27. Ishikawa M, Kusaka G, Yamaguchi N, et al. Platelet and leukocyte adhesion in the microvasculature at the cerebral surface immediately after subarachnoid hemorrhage. *Neurosurgery* 2009; 64: 546–553.
28. Sehba FA, Schwartz AY, Chereshnev I, et al. Acute decrease in cerebral nitric oxide levels after subarachnoid hemorrhage. *J Cereb Blood Flow Metabolism* 2000; 20: 604–611.
29. Sun BL, Zhang SM, Xia ZL, et al. L-arginine improves cerebral blood perfusion and vasomotion of microvessels following subarachnoid hemorrhage in rats. *Clin Hemorheol Microcirc* 2003; 29: 391–400.
30. Koide M, Dunn KM, Bulkeley EA, et al. In vivo and ex vivo dysfunction of neurovascular coupling in a mouse model of subarachnoid hemorrhage. *FASEB* 2014; 28: 676.
31. Sehba FA, Friedrich V Jr, Makonnen G, et al. Acute cerebral vascular injury after subarachnoid hemorrhage and its prevention by administration of a nitric oxide donor. *J Neurosurg* 2007; 106: 321–329.
32. Pappas AC, Koide M and Wellman GC. Purinergic signaling triggers endfoot high-amplitude Ca^{2+} signals and causes inversion of neurovascular coupling after subarachnoid hemorrhage. *J Cereb Blood Flow Metabolism* 2016; 36(11): 1901–1912.